Metal Oxides

DOI: 10.1002/anie.201204884

Impact of Crystal Chemistry upon the Physics of Strongly Correlated Electrons in Oxides

*Bernard Raveau**

cobaltates · colossal magnetoresistance · cuprates · manganates · superconductors

The numerous studies that were performed these last twenty five years on strongly correlated electrons in oxides have shown that they represent a great potential for applications as functional materials. This is the case of high critical temperature (T_c) superconducting cuprates which are of high interest in electronic applications, but also in high-current applications for saving energy, and as magnetic bearings. Similarly, oxides have been investigated for their potential as magnetic memory materials and actuators, as for example in the studies of colossal magnetoresistance manganates, and of many other oxides, called multiferroics which combine both ferroelectricity and ferromagnetism. A third example is given by the thermoelectric cobaltates, which exhibit good performances at high temperature and offer a possible solution for saving energy by conversion of waste heat into electricity. In fact, transition-metal oxides were considered for a long time as inadequate materials for investigation by physicists, owing to their too complex crystal chemistry. The discovery of superconductivity at "high temperature" by Bednorz and Müller in 1986[1] in one cuprate of the "La-Ba-Cu-O" system has shown the opposite, since a new superconductor with a critical temperature much higher than that observed previously in more simple systems was born from this investigation. Indeed, a T_c of 38 K was observed for the first time, much higher than that of Nb_3Ge of 23 K, which was considered by a majority of physicists as an upper limit which could not be overpassed. Such a discovery was made possible because Bednorz and Müller took into consideration for their exploration, previous results on the crystal chemistry of cuprates in spite of their complexity, and more particularly, the existence of the cuprate $La_4BaCu_5O_{13}$ that had been shown to be a perovskite derivative with an exotic metallic conductivity.[2] Clearly, the metallic conductivity is necessary but not sufficient for the appearance of superconductivity. To generate metallic conductivity in transition-metal oxides, the solid-state chemist has generally to consider the possible delocalization of charge carriers (electrons or holes) in a band system mainly built up from the overlap of the p orbitals of the oxygen atoms and d orbitals of the transition element implying for the transition element a mixed valence. In the case of copper oxides, the charge carriers are holes, corresponding to the mixed-valence Cu^{II}–Cu^{III}, so that the stabilization of Cu^{III} at normal pressure was absolutely necessary for the synthesis of new metallic conductors. This condition could be fulfilled by introducing alkaline-earth cations, such as Ba^{2+}, Sr^{2+}, or Ca^{2+}, as well as the trivalent lanthanide cation in the Ln-Cu-O system.[3] In this way a series of mixed-valent cuprates, all exhibiting a metallic conductivity, such as $La_{2-x}A_xCuO_4$ (A = Ca,Sr), $La_{2-x}(Sr,Ca)_{1+x}Cu_2O_6$, $La_4BaCu_5O_{13}$, had been synthesized several years before the discovery of high T_c superconductivity. Then, the choice of the compound for the investigation of superconductivity was not straightforward, and we know today that the decision to investigate $La_4BaCu_5O_{13}$ was going in the wrong direction. Indeed, it is now established that superconductivity in cuprates requires bidimensional carrier correlations, that is, the existence of "disconnected" copper–oxygen layers, whereas in contrast, three-dimensional carrier correlations suppress the superconducting effect. For this reason, the structure of $La_4BaCu_5O_{13}$ (Figure 1a), built up of corner sharing CuO_5 pyramids and CuO_6 octahedra, which implies a 3D overlap of the 3d-Cu orbitals and 2p-O orbitals, cannot exhibit any superconductivity. Fortunately, the composition prepared and studied by Bednorz and Müller was a mixture of this oxide and of another cuprate, $La_{2-x}Ba_xCuO_4$,[3] whose structure (Figure 1b) consists of perovskite copper monolayers stacked with single rock salt

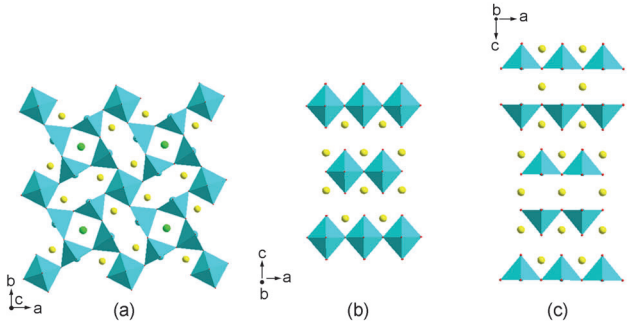

Figure 1. Structures of the cuprates a) $La_4BaCu_5O_{13}$, in which the corner-shared CuO_5 pyramids and CuO_6 octahedra form a 3D framework (La^{3+} yellow spheres, Ba^{2+} green spheres), b) $La_{2-x}Ba_xCuO_4$, in which the CuO_6 octahedra form single perovskite layers interleaved with $La_{1-x}Ba_xO$ single rock-salt layers (Ba^{2+}, La^{3+} yellow spheres), c) $La_{2-x}(Sr,Ca)_{1+x}Cu_2O_6$ built up of double layers of corner-shared CuO_5 pyramids (La, Sr, Ca yellow spheres).

[*] Prof. B. Raveau
CRISMAT, ENSICAEN-CNRS UMR 6508
6 bd. Maréchal Juin, 14050 Caen (France)
E-mail: bernard.raveau@ensicaen.fr

layers $(La_{1-x}Ba_x)O$. It is then the presence of this layered cuprate, which associates both the mixed valence of copper and bidimensionality of the electron correlations in the structure, which was responsible for the existence of superconductivity in the sample of nominal composition "$La_4BaCu_5O_{13}$".

Bearing in mind the crucial role of the structure bidimensionality for the appearance of superconductivity, another parameter, the Jahn–Teller effect of copper was then revealed to be the key for the realization of new layered superconductive cuprates. It is well established for the solid-state chemist that the Jahn–Teller effect of copper favors the formation of CuO_5 pyramids and of CuO_4 square-planar groups instead of CuO_6 octahedra. Based on this consideration, it was possible, in 1980,[3] before the superconductivity rush, to convert double octahedral perovskite layers into double layers of corner-sharing CuO_5 pyramids, leading to the layered cuprate $La_{2-x}(Sr, Ca)_{1+x}Cu_2O_6$ (Figure 1c), which was found ten years later to be a 60 K superconductor.[4] Then, the discovery in 1987 of superconductivity at 92 K in the Y-Ba-Cu-O system,[5] where the structure of $YBa_2Cu_3O_7$ (Figure 2)

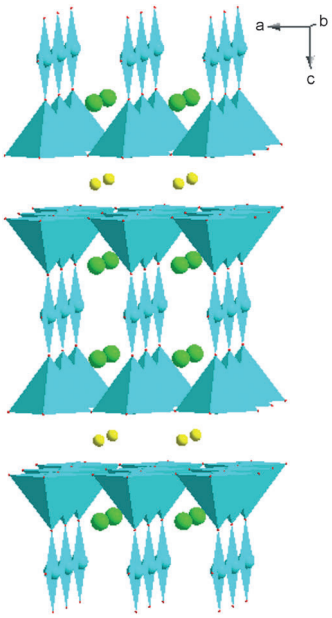

Figure 2. Structure of $YBa_2Cu_3O_7$ showing double layers of CuO_5 pyramids interleaved with Y^{3+} ions (yellow spheres) and interconnected through rows of CuO_4 square planar groups; Ba^{2+} green spheres.

was shown to exhibit double layers of CuO_5 pyramids interconnected through rows of CuO_4 square planar groups,[6,7] was a strong indication of the important role of multiple but "disconnected" copper layers for increasing T_c. The possibility to introduce "Bi_2O_2" layers for the synthesis of lamellar superconducting cuprates was demonstrated as early as 1987, with the discovery of superconductivity at 22 K in the Bi-Sr-Cu-O system.[8] The exploration of this system was based on the fact that, because of the presence of the $6s^2$ electronic lone pair of Bi^{3+}, a large series of layered oxides, called Aurivillius phases,[9] had been synthesized with a structure built of "$A_{n-1}B_nO_{3n+1}$" perovskite layers (A = Ca, Sr, Pb, Bi, Ba; B = Ti, Nb, Ta) interleaved with "Bi_2O_2" layers. Effectively, the structure of the 22 K superconductor $Bi_2Sr_2CuO_{6+\delta}$ (where δ represents additional oxygen that can be inserted into the "Bi_2O_2" layers, depending on the method of synthesis; Figure 3a) consists of single copper perovskite layers intergrown with $Bi_2Sr_2O_4$ layers, themselves

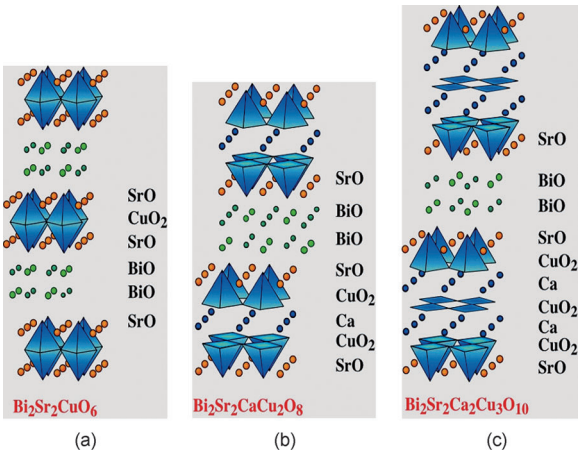

Figure 3. Schematic structures of the bismuth cuprates
a) $Bi_2Sr_2CuO_{6+\delta}$ built up of single octahedral copper layers
b) $Bi_2Sr_2CaCu_2O_{8+\delta}$ built up of double pyramidal copper layers
c) $Bi_2Sr_2Ca_2Cu_3O_{10+\delta}$ built up of triple copper layers.

built of "Bi_2O_2" layers sandwiched between two "SrO" planes. This study opened the road to the investigation of other bismuth-based cuprates, leading to a dramatic increase of the critical temperature up to 88 K and 110 K in the Bi-Sr-Ca-Cu-O system,[10,11] corresponding to the cuprates $Bi_2Sr_2CaCu_2O_{8+\delta}$ and $Bi_2Sr_2Ca_2Cu_3O_{10+\delta}$ respectively. The numerous crystal studies of these two bismuth cuprates (see for a Review Ref. [12]), showed definitively that the Jahn–Teller effect of copper is absolutely necessary for the stabilization of their structure, leading to the formation of double copper layers of CuO_5 corner-sharing pyramids in $Bi_2Sr_2CaCu_2O_{8+\delta}$ (Figure 3b) and triple copper layers formed of one median layer of CuO_4 square-planar groups sandwiched between two layers of CuO_5 pyramids in $Bi_2Sr_2Ca_2Cu_3O_{10+\delta}$ (Figure 3c).

Thus, from the crystal chemistry of these cuprates it appeared that two important features govern superconductivity in these materials: the multiplicity of the copper layers and the chemical nature of the non-copper layers. The increase of T_c from 22 K to 110 K as the multiplicity of the copper layers increases from $n = 1$ to $n = 3$, is a remarkable feature, whose origin is to date still a matter of debate. The possibility to reach so high values of T_c compared to $La_{2-x}A_xCuO_4$ or to $La_{2-x}(Sr,Ca)_{1+x}Cu_2O_6$, emphasizes the influence of the bismuth–oxygen layers upon superconductivity, showing that they play the role of hole reservoirs with respect to the copper–oxygen layers. Then, the discovery in 1988, of superconductivity in the Tl-Ba-Cu-O and Tl-Ba-Ca-Cu-O systems up to 125 K[13] allowed numerous superconductive oxides, with a layered structure closely related to

those of the bismuth cuprates, to be synthesized (see for a Review ref. [12]), as exemplified for the superconductor $Tl_2Ba_2Ca_2Cu_3O_{10}$, which exhibits the highest T_c, with a structure very similar to that of $Bi_2Sr_2Ca_2Cu_3O_{10+\delta}$, double "$Tl_2O_2$" layers replacing "$Bi_2O_2$" layers. The discovery of high T_c superconducting mercury cuprates in 1993 was based on the particular linear two-fold coordination of mercury, leading to the 96 K superconductor $HgBa_2CuO_4$,[14] whose structure (Figure 4) consists of single perovskite octahedral layers interconnected through single layers of HgO_2 dumbbells. The

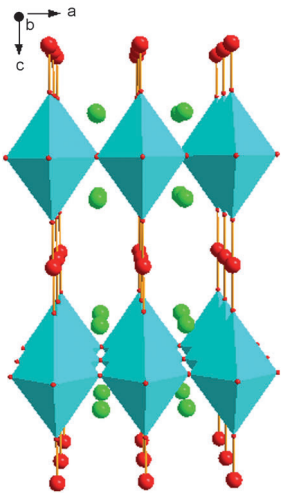

Figure 4. Structure of the cuprate $HgBa_2CuO_4$ (Hg red spheres; Ba^{2+} green spheres).

T_c was later increased to 120 K for $HgBaCa_2Cu_2O_6$[15] and to 135 K[16] by replacing the single copper layers by double and triple copper layers respectively, similar to bismuth and thallium cuprates (for a Review, see Ref. [12]).

Besides its role for the generation of new superconductors, the crystal chemistry of copper oxides has also a great impact upon the optimization of their properties and the understanding of the physics of these materials. Thousands of papers were published about the role of oxygen stoichiometry upon the transport properties of cuprates, as for example, the oxygen excess in the bismuth–oxygen layers of the bismuth cuprates, or the oxygen deficiency in the $YBa_2Cu_3O_7$-type structure, or the cationic deficiency and disordering in the "TlO" layers of the thallium cuprates. In the same way, the detailed structure of these oxides, such as structural distortions, or commensurate and incommensurate modulations as in bismuth cuprates, were also observed to be key parameters for the interpretation of the physics of these compounds.

The discovery of high T_c superconductivity in cuprates has then served as a stepping stone for the studies of correlated dynamics of spins and charges in other transition-metal oxides involving strong electron correlations. This is the case of the manganates $Ln_{1-x}A_xMnO_3$ (Ln = lanthanide, A = Ca, Sr, Ba, Pb) which have long been known to have the perovskite structure and mixed valence Mn^{III}–Mn^{IV} leading to promising magnetic and transport properties.[17] After the pioneer work of Kusters et al.[18] showing large magnetoresistance (MR) effects, these systems were revisited by several groups almost simultaneously, showing huge MR effects, called colossal magnetoresistance (CMR).[19–23] The huge decrease of resistance that appears in those oxides by applying a magnetic field corresponds to a transition from a paramagnetic or antiferromagnetic insulating state to a ferromagnetic metallic state. Thus, like for high T_c cuprates, CMR manganates require metallic conductivity, and consequently the presence of the mixed valence Mn^{III}–Mn^{IV}. However this time, the metallic state must also be ferromagnetic, requiring a different mechanism called double exchange,[24,25] where the spins of the charge carriers are parallel to the local ionic spins, and do not change their orientation when moving. Unlike the cuprates, the mixed-valent manganese perovskites are, in most cases stoichiometric and the oxygen deficiency is not an important parameter for the appearance of the CMR effect. In the same way, contrary to the cuprates, the bidimensionality of the structure is not required for the generation of the effect. In contrast, it was shown early on, that like for the cuprates, the Jahn–Teller effect of Mn^{3+} plays a crucial role in the CMR properties.

The first class of manganates involving the CMR effect are those which exhibit a transition from a paramagnetic insulating state to a ferromagnetic metallic state as the temperature is decreased or as a magnetic field is applied. This is exemplified by the manganates $Pr_{0.7}(Ca, Sr)_{0.3}MnO_3$[26] for which spectacular drops of the resistivity, up to 11 orders of magnitude in a field of 5 T at 30 K (Figure 5), were observed. The neutron diffraction study of one of these

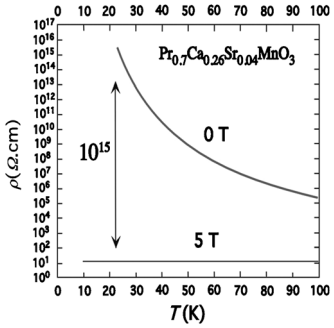

Figure 5. Spectacular drop of resistivity under a magnetic field of 5 T in the perovskite $Pr_{0.7}Ca_{0.26}Sr_{0.04}O_3$.

compounds, $Pr_{0.7}Ca_{0.2}Sr_{0.1}MnO_3$,[27] demonstrated clearly that, although the symmetry of the structure does not change, the transition from the paramagnetic insulating state to the ferromagnetic metallic state at $T_C \approx 150$ K (Figure 6a) is accompanied by an abrupt decrease of the orthorhombic distortion as T decreases corresponding to an abrupt decrease of the Jahn–Teller distortion of the MnO_6 octahedra at T_C (Figure 6b). Thus, the existence of strong correlations between the Jahn–Teller distortion and the magnetic ordering of manganese was shown for the first time, suggesting that the appearance of the ferromagnetic metallic state requires the formation of Mn-O-Mn angles as close as possible to 180° to favor a better overlapping of the Mn-3d and O-2p orbitals. The effect of the size of the A-site cation upon the para-

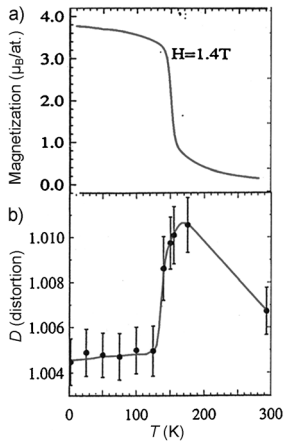

Figure 6. $Pr_{0.7}Ca_{0.2}Sr_{0.1}MnO_3$: a) transition from the paramagnetic to the ferromagnetic state at $T_C \approx 150$ K. b) Abrupt decrease of the Jahn–Teller distortion "*D*" at the MnO_6 octahedra at T_C ($D = d\text{Mn–O}_{apical}/d\text{Mn–O}_{equatorial}$)

magnetic insulator to ferromagnetic metal transition, and consequently upon the CMR effect described by many authors [for see Reviews Ref. [28,29]] is then, dictated by the Jahn–Teller effect of Mn^{3+}. Indeed, the size of the A cations in the perovskite cages influences dramatically the structural distortion of the MnO_6 octahedra in the paramagnetic state and consequently governs the structural transition to a more symmetric ferromagnetic metallic structure, by decreasing the temperature or by applying a magnetic field.

The second class of CMR manganates is represented by compounds which exhibit a transition from an antiferromagnetic insulating state to a ferromagnetic metallic state on decreasing the temperature or, under a magnetic field, as shown for the first time in 1995 for $Pr_{1/2}Sr_{1/2}MnO_3$[30] and for $Pr_{1-x}Ca_xMnO_3$.[31] The CMR effect of these materials is based on the existence of charge ordering at low temperature in the antiferromagnetic insulating state, a structural feature which was revealed in 1980s,[32] a long time before the discovery of the CMR effect. In fact, this important characteristic for CMR properties has its origin in the Jahn–Teller effect of Mn^{3+}, as illustrated from the antiferromagnetic 1:1 charge ordering of Mn^{3+} and Mn^{4+} in $Pr_{0.5}Ca_{0.5}MnO_3$ (Figure 7a) which consists of single ribbons of strongly elongated $Mn^{III}O_6$ octahedra alternating with single ribbons of practically regular $Mn^{IV}O_6$ octahedra. Thus, here again, the Jahn–Teller effect of Mn^{3+} is responsible for the insulating and antiferromagnetic behavior of $Pr_{0.5}Ca_{0.5}MnO_3$, and charge ordering can only be achieved by applying a very high magnetic field, over 25 Tesla, to obtain a more symmetric perovskite structure (Figure 7b), with a ferromagnetic metallic state. Then, it is easy to understand that different thicknesses of the regular Mn^{IV} octahedral perovskite blocks can be obtained by varying *x* in the $Pr_{1-x}Ca_xMnO_3$ oxides, so that the transition temperature, or the critical value of the magnetic field will depend on the crystal structure of these oxides and namely on the nature of charge ordering (see for Reviews Refs. [28,29]).

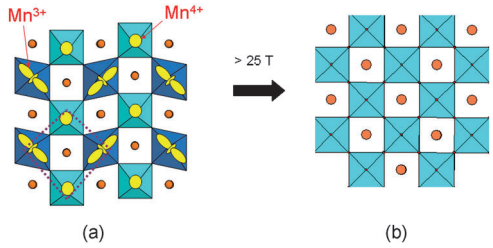

Figure 7. $Pr_{0.5}Ca_{0.5}MnO_3$: Transition from the orthorhombic Jahn–Teller distorted antiferromagnetic (a) to the ferromagnetic more symmetric structure (b) under a magnetic field greater than 25 T. The magnetic field changes the elongated Mn^{3+} octahedra (dark blue in (a)) into more symmetric Mn^{3+}/Mn^{4+} octahedra (light blue in (b)).

Thus, the crystal structure, or more exactly the Jahn–Teller distortion of Mn^{3+}, is the crucial parameter which is the origin of the CMR effect in manganates and it can be controlled by tuning the size of the A site cations in the perovskite cages and or by varying the Mn^{3+}/Mn^{4+} ratio on the basis of different kinds of charge ordering. The Jahn–Teller effect and consequently the CMR effect can also be controlled by local structural effects. This was demonstrated by the size-mismatch effect σ^2,[33] which shows that the simultaneous presence of Ln^{3+} ions of different sizes in the perovskite cages affects the CMR properties of these materials, with T_C decreasing as the size-difference increases, for a constant average size of the A site cations.

A very efficient method is doping at the Mn sites or at the A site which can be used to induce the ferromagnetic metallic state, or to lower the critical field for obtaining the CMR effect. This approach was demonstrated for the first time by doping the Mn sites of the antiferromagnetic insulator $Pr_{0.5}Ca_{0.5}MnO_3$ with less than 6% Cr^{3+},[34] leading to CMR effect and even to a transition from the antiferromagnetic insulating state to the ferromagnetic metallic state (Figure 8). This spectacular doping effect can be explained by the fact that locally, one Mn^{3+} Jahn–Teller distorted octahedron is replaced by one perfectly regular Cr^{3+} octahedron, so that the structure around it becomes more symmetric, close to that of a cubic perovskite (Figure 9a), forming ferromagnetic metallic islands, in the antiferromagnetic insulating matrix of $Pr_{0.5}Ca_{0.5}MnO_3$ (Figure 10a) which exhibits a different orthorhombic symmetry. Thus, a phase separation scenario could

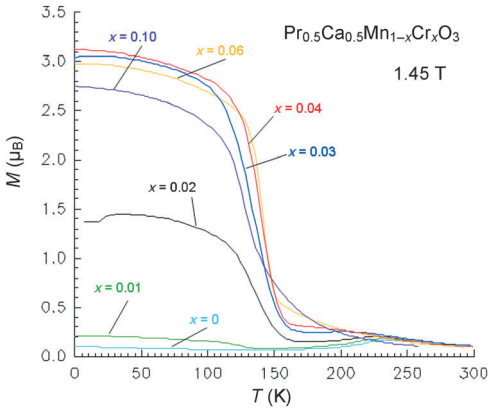

Figure 8. Transition from the antiferromagnetic state to the ferromagnetic state by doping $Pr_{0.5}Ca_{0.5}MnO_3$ with chromium.

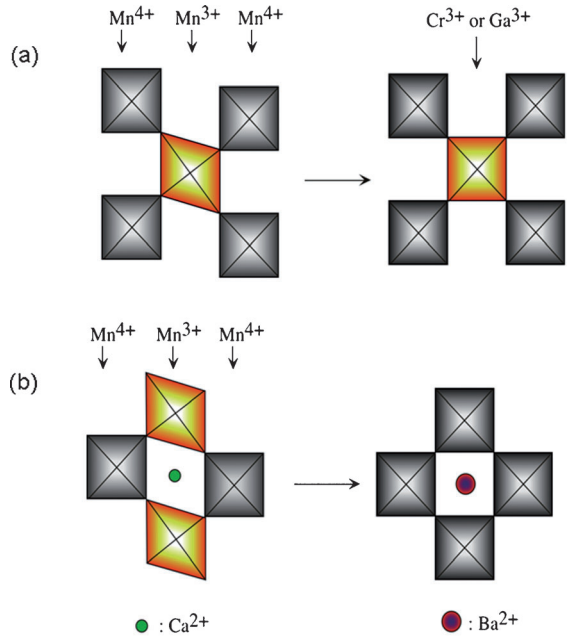

Figure 9. Increase of the local symmetry of the perovskite structure by doping a) the Mn^{3+} site with non Jahn–Teller Cr^{3+} ion and b) the A site (Ca^{2+}) by a larger Ba^{2+} ion.

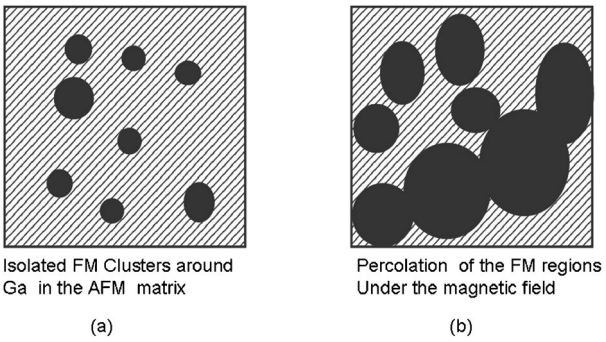

Figure 10. Phase-separation scenario of the transition from antiferromagnetic (AFM) insulating to ferromagnetic (FM) metallic state obtained by Cr (or Ga) doping and at increasing magnetic field in $Pr_{0.5}Ca_{0.5}MnO_3$.

be proposed [for a Review see Ref. [35]], where the ferromagnetic islands extend in the antiferromagnetic matrix as the Cr content is increased (Figure 10b), but also as the applied magnetic field increases, so that percolation of these domains occurs. In this particular case of Cr^{3+} doping, the presence of a magnetic field is even not necessary to form the ferromagnetic metallic state, because the local antiferromagnetic coupling of Cr^{3+} with its next manganese neighbors (Figure 11) induces a reversal of the spins of the antiferromagnetic structure in the pure manganite, leading to a ferromagnetic structure by a domino effect in the Cr-doped phase.[36] The electronic-magnetic phase-separation scenario, was also applied to the doping of the Mn^{3+} sites by other nonmagnetic and non Jahn–Teller cations, such as Ga^{3+} [35,38] or magnetic cations, such as Ru^{4+},[37] showing that the application of a magnetic field to these doped manganates leads to ultra-sharp steps in the magnetization (Figure 12a)

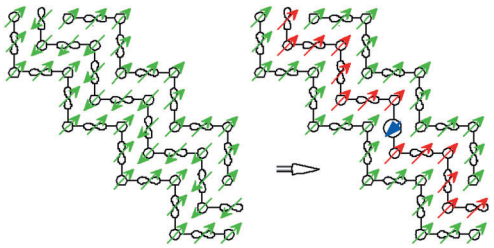

Figure 11. Reversal of the spins of the antiferromagnetic structure of $Pr_{0.5}Ca_{0.5}MnO_3$ (left) to a ferromagnetic structure (right) by Cr doping. The local antiferromagnetic coupling of Cr spin (blue) with next neighbors Mn spins (green and red) leads to ferromagnetism by a domino effect.

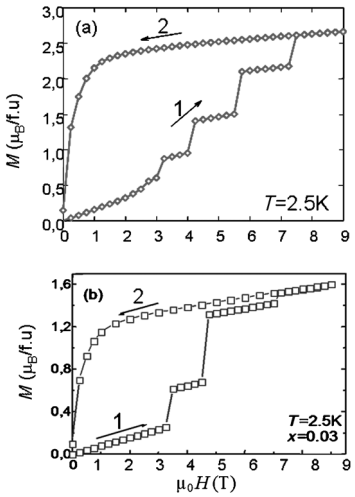

Figure 12. Ultra-sharp magnetization steps (1) induced by doping a) with Ga at the Mn sites and b) with Ba at the A sites.

and the resistivity under a magnetic field.[38] Based on the phase-separation scenario, this phenomenon was explained by a martensitic mechanism[38] in that the ferromagnetic metallic domains and the antiferromagnetic insulating matrix exhibit a different crystal-structure symmetry and develop strains at their interfaces. These strains are overcome by increasing the applied magnetic field. The doping at the A site also induces the formation of ultra-sharp magnetization steps[39] as shown for example for the Ba-doped $Pr_{0.5}Ca_{0.5}MnO_3$ (Figure 12b). It is also explained by the martensitic mechanism. In fact, the introduction of Ba^{2+} ions, which are much larger than the Ca^{2+} ions, to the A sites, also develops more symmetric perovskite islands (Figure 9b) in the orthorhombic antiferromagnetic matrix of $Pr_{0.5}Ca_{0.5}MnO_3$, decreasing and even destroying locally the Jahn–Teller effect of Mn^{3+}, then such ferromagnetic domains can extend by increasing the magnetic field, similarly to the Mn-site doping (Figure 10).

From all the investigations that have been carried out in CMR manganates, it is clear that the impact of crystal chemistry and especially of the structural distortions arising from the Jahn–Teller effect of Mn^{3+} upon the physics of these materials is considerable, so that the Mn^{III}–Mn^{IV} mixed-valence, the size of the A cations, their size difference (size

mismatch), and the doping at the Mn and A sites are the main parameters that can be used for the control of magnetism and magnetotransport properties of these perovskites.

The spectacular discoveries that were made for copper and manganese oxides have stimulated investigations of other strongly electron-correlated oxides. In this respect, cobalt oxides represent a vast field for research, all the more as the crystal chemistry and magnetism are more complicated with the existence for cobalt of several oxidation states—Co^{II}, Co^{III}, Co^{IV}—several coordination geometries—octahedral, tetrahedral, pyramidal—and several spin states—high (HS), intermediate (IS), and low spin (LS). Numerous studies have then been carried out, showing very attractive results in these strongly electron-correlated systems which cannot all be covered herein (for a Review see Ref. [40]). A first example is given by the discovery of the exceptionally high magnetoresistance associated with a metal–insulator transition around room temperature (Figure 13) in the ordered oxygen deficient "112" perovskites $LnBaCo_2O_{5.5+\delta}$, with Ln = Eu, Gd.[41] This

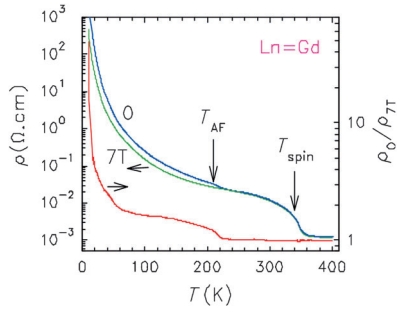

Figure 13. Metal–insulator transition (under 0T and 7T) and high magnetoresistance in the "112" perovskite $LnBaCo_2O_{5.5+\delta}$.

result opened the route to numerous studies of complex magnetic and transport properties of these compounds (for a Review, see Section 3 of Ref. [40]). In fact, the crystal structure of this phase (Figure 14), built up of octahedral perovskite layers and interconnected through ribbons of CoO_5 pyramids, generates complex oxygen non-stoichiometry phenomena. Consequently, the variation of the oxygen content δ, dramatically influences the magnetic and transport properties of these oxides, by changing the cobalt valence, which may vary from the formal trivalent state ($\delta = 0$), to

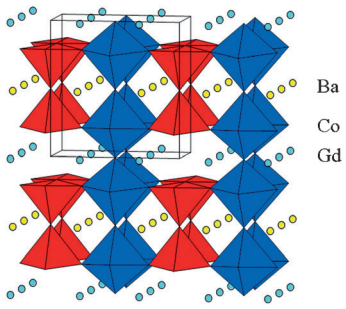

Figure 14. Crystal structure of the "112" $GdBaCo_2O_{5.5}$ cobaltite, built up of CoO_5 pyramids and CoO_6 octahedra

mixed-valence states Co^{2+}/Co^{3+} ($\delta < 0$) and Co^{3+}/Co^{4+} ($\delta > 0$) and may even exhibit a disproportionation of Co^{3+} into Co^{2+} and Co^{4+}. Concomitantly, the spin states of cobalt change, leading to various magnetic interactions, to various electronic properties, and to phase separation similar to that found in manganates. High magnetoresistance effects are not limited to this structural type, but are also observed for other perovskite cobaltates and also derivatives, such as Ruddlesden and Popper-type phases. Again, all these oxides often exhibit a large oxygen deficiency with respect to the ideal formula $ACoO_3$ and the relationships between the chemistry and the physics of these oxides are still in many cases, a matter of debate.

The thermoelectric cobaltates are the second example of strongly electron-correlated cobaltates. The discovery of a high figure of merit at high temperature for the cobaltate Na_xCoO_2[42] was clearly based on the work performed 24 years earlier on this oxide.[43] It was indeed known, as early as 1973, that Na_xCoO_2, which has a layered structure with a triangular geometry, built up of octahedral "CoO_2" layers (Figure 15), shows a high conductivity, together with a high thermoelectric power at room temperature.[43] From the above considera-

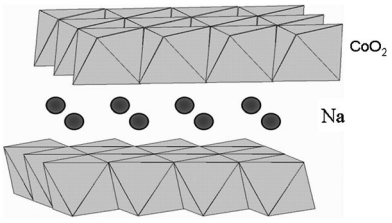

Figure 15. Layered structure of Na_xCoO_2, built up of "CoO_2" layers of edge-sharing CoO_6 octahedra interleaved with Na^+ ions.

tions of strongly correlated electrons in oxides, it is clear that the high p-type conductivity of this cobaltate requires the mixed-valence Co^{III}–Co^{IV} but this alone is not sufficient, because the magnetic ordering is generally strong in cobalt oxides. In this case, two crystal factors contribute to the simultaneous decrease of resistivity and to the increase of the thermoelectric power: the layered character of the structure and the triangular geometry of the cobalt sublattice. It results in the splitting of the t_{2g} orbitals of cobalt, leading to a narrow a_{1g} band overlapping with a broader e'_g band. Consequently, the holes in the e'_g band are responsible for the metal-like conductivity, whereas the large density of states at the Fermi level leads to large thermoelectric power values. Thus, Na_xCoO_2 exhibits at high temperature, $T \approx 900$–1200 K, a low resistivity $\rho \approx 2 \times 10^{-4}$ Ωcm, and a high thermoelectric power $S \approx 100\ \mu V K^{-1}$,[42,43] allowing a good figure of merit $ZT = (S^2/\rho k)T$, where k is the thermal conductivity, to be obtained. The low value of k in this oxide, seems to originate from cationic disordering of the Na^+ ions between the "CoO_2" layers. The large series of misfit cobaltates, that were discovered in the systems "Tl-Sr-Co-O" and "Bi-Sr-Co-O",[44] were then explored extensively for their very attractive thermoelectric properties (for a Review see Section 6 of Ref. [40]). In fact, the structure of these oxides is closely

related to that of Na_xCoO_2 on one side and to those of the cuprates on the other side, as illustrated for the misfit $(Bi_{0.87}SrO_2)_2(CoO_2)_{1.82}$ (Figure 16), which structure exhibits "CoO_2" layers similar to Na_xCoO_2, stacked with rock-salt type layers "$Bi_{1.74}Sr_2O_4$" similar to the bismuth cuprates. Their

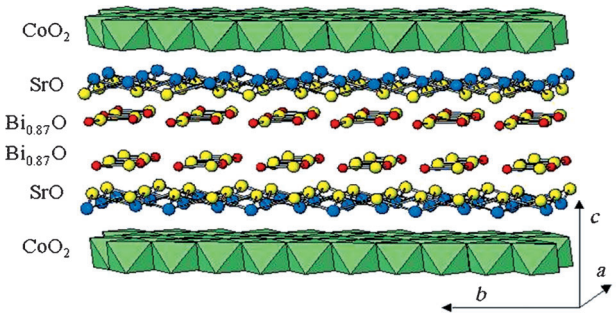

Figure 16. Structure of the misfit cobaltite $(Bi_{0.87}SrO_2)_2(CoO_2)_{1.82}$ built up of "CoO_2 octahedral layers interleaved with rock salt-like "$Bi_{1.74}Sr_2O_4$" layers.

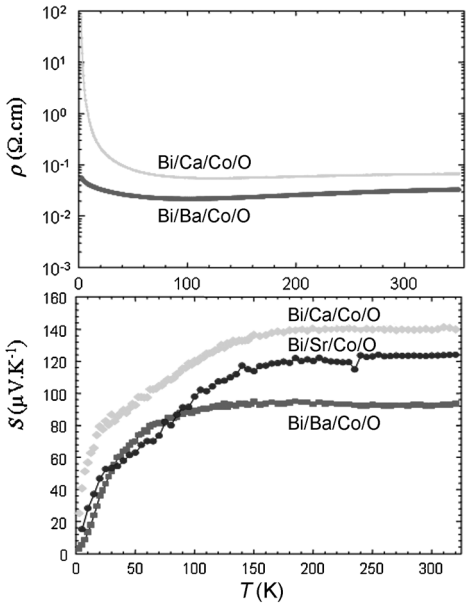

Figure 17. Resistivity ρ and thermoelectric power S versus temperature T for several bismuth-based misfit cobaltites.

crystal chemistry, then allows all three conditions to be fulfilled: cobalt mixed valence, triangular geometry of the cobalt sublattice, and bidimensionality of the structure, so that these misfits exhibit enhanced thermoelectric power values up to 140 $\mu V K^{-1}$ as shown for the bismuth cobaltate (Figure 17).[44]

Cobalt oxides were also recently shown to be a potential source of multiferroic materials. The orthorhombic cobaltate $CaBaCo_4O_7$[45] is indeed one of the rare multiferroic materials which is ferrimagnetic. This mixed-valent Co^{II}–Co^{III} oxide, exhibits a pure tetrahedral structure (Figure 18) involving a complex ordering of the Co^{2+} and Co^{3+} cations, which is at the origin of its ferrimagnetic properties below 60 K. Importantly, it was observed that this "114" cobaltite exhibits a unique symmetry point group m′m2′, in which ferroelectricity, ferromagnetism, and ferrotoroidicity are allowed. All three vectors—polarization, magnetization, and torodization—are perpendicular, suggesting multiferroic properties. Dielectric and polarization measurements performed on this oxide[45] confirmed this hypothesis, showing a clear peak on the $\varepsilon'(T)$ curve at T_C, which was found frequency independent. Polarization measurements under a magnetic field of $+111\ kV m^{-1}$ versus temperature showed a constant value of approximately 75 $\mu C m^{-2}$ in the range 45–40 K, with a broad transition beyond 40 K polarization tending towards zero at T_C (Figure 19a), whereas the symmetric curve was observed by applying a negative magnetic field of $-111\ kV m^{-1}$. The $\Delta\varepsilon'/\varepsilon$ (H) curves at various temperatures (Figure 19b) showed that a maximum magnetodielectric effect of approximately 16% could be reached around T_C. Thus, these results show the great impact of crystal chemistry upon the coupling of ferrimagnetism and ferroelectricity in the multiferroic oxides, paving the way for the exploration of new possible magnetic effects in the "114" family.

In conclusion, the crystal chemistry of transition-metal oxides has opened a wide avenue for the exploration of strongly correlated electron systems. There is no doubt that the physics of these materials, especially magnetism and electronic properties, is closely dependent on their chemistry and complex phenomena, such as electronic or magnetic phase separation, or charge-orbital ordering, can only be understood and controlled on the basis of oxygen non-stoichiometry, the Jahn–Teller effect, and other structural distortions, as well as order–disorder phenomena. It is also

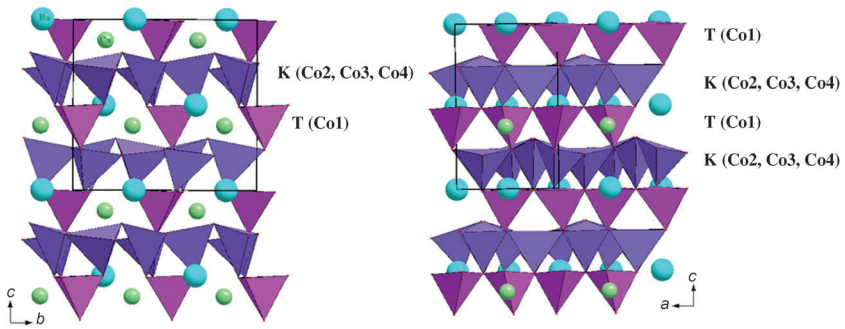

Figure 18. Tetrahedral structure of the "114" orthorhombic cobaltite $CaBaCo_4O_7$ showing charge ordering of Co^{3+} and Co^{2+} species (Co^{2+} = Co2, Co3; Co^{3+}/Co^{2+} = Co1, Co4). Blue spheres = Ba^{2+}, green spheres = Ca^{2+}, pink tetrahedra = triangular layers and purple tetrahedra = kagomé layers.

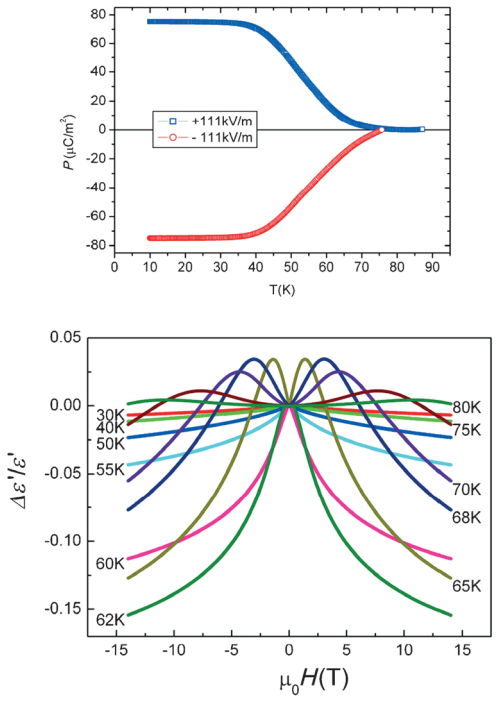

Figure 19. Multiferroic properties of $CaBaCo_4O_7$: a) temperature dependence of electric polarization $P(E{=}111\ kV\,m^{-s})$ showing a clear transition at T_C and a change of sign of P by reversing E. b) Relative dielectric permittivity at 100 kHz as a function of magnetic field for different temperatures.

worth emphasizing that these studies have a great impact upon the realization and optimization of materials for various applications, particularly in the fields of energy, as for high T_c superconductors and thermoelectics, and of memory storage, as for magnetoresistive and multiferroic oxides.

Received: June 22, 2012
Published online: December 3, 2012

[1] J. G. Bednorz, K. A. Müller, *Z. Phys. B* **1986**, *64*, 189.
[2] C. Michel, L. Er-Rakho, B. Raveau, *Mater. Res.* **1985**, *20*, 667.
[3] N. Nguyen, C. Michel, F. Studer, B. Raveau, *Mater. Chem.* **1982**, *7*, 413; N. Nguyen, C. Michel, F. Studer, B. Raveau, *J. Phys. Chem. Solids* **1983**, *44*, 389; C. Michel, B. Raveau, *Rev. Chim. Miner.* **1984**, *21*, 407; N. Nguyen, L. Er-Rakho, C. Michel, J. Choisnet, B. Raveau, *Mater. Res. Bull.* **1980**, *15*, 891.
[4] R. J. Cava, B. Battlog, R. B. Van Dover, J. J. Krajewski, J. W. Wasczak, R. M. Fleming, W. F. Peck, L. W. Rupp, P. Marsh, A. C. James, L. F. Schneemeyer, *Nature* **1990**, *345*, 602.
[5] M. K. Wu, J. R. Ashburn, C. J. Torng, P. H. Hor, R. L. Meng, L. Gao, T. J. Huang, Y. Z. Wang, C. W. Chu, *Phys. Rev. Lett.* **1987**, *58*, 908.
[6] M. A. Beno, L. Soderholm, D. W. Capone, D. Hinks, J. D. Jorgensen, I. K. Schuller, C. U. Segre, K. Zhang, J. D. Grace, *Appl. Phys. Lett.* **1987**, *51*, 57.
[7] J. Capponi, C. Chaillout, A. W. Hewat, P. Lejay, M. Marezio, N. Nguyen, B. Raveau, J. L. Soubeyroux, J. L. Tholence, R. Tournier, *Europhys. Lett.* **1987**, *12*, 1301.
[8] C. Michel, M. Hervieu, M. M. Borel, A. Grandin, F. Deslandes, J. Provost, B. Raveau, *Z. Phys. B* **1987**, *68*, 421.
[9] B. Aurivillius, *Ark. Kemi* **1949**, *1*, 463; B. Aurivillius, *Ark. Kemi* **1949**, *1*, 499; B. Aurivillius, *Ark. Kemi* **1950**, *2*, 519; B. Aurivillius, *Ark. Kemi* **1952**, *5*, 39.
[10] H. Maeda, J. Tanaka, M. Fukutomi, T. Asano, *Jpn. J. Appl. Phys.* **1988**, *27*, L209.
[11] N. Mizuno, U. Endo, J. Tschuchiya, N. Kijima, A. Sumiyama, Y. Oguri, *Jpn. J. Appl. Phys. P* **1988**, *27*, L1225; U. Endo, S. Koyama, T. Kawai, *Jpn. J. Appl. Phys.* **1988**, *27*, L1476.
[12] "*Ruddlesden and Popper—Phases and Derivatives: Homologous series of Transition Metal Oxides*": B. Raveau, *Comprehensive Inorganic Chemistry II*, New Age International, Darya Ganj, **2012**.
[13] Z. Z. Sheng, A. M. Hermann, *Nature* **1988**, *332*, 55; Z. Z. Sheng, A. M. Hermann, *Nature* **1988**, *332*, 138.
[14] S. N. Putilin, E. V. Antipov, M. Marezio, *Nature* **1993**, *362*, 226.
[15] P. G. Radaelli, J. L. Wagner, B. A. Hunter, M. A. Beno, G. S. Knapp, J. D. Jorgensen, *Physica C* **1993**, *216*, 29; Q. Huang, J. W. Lynn, R. L. Mang, C. W. Chu, *Physica C* **1993**, *218*, 356.
[16] O. Chmaissem, Q. Huang, E. V. Antipov, S. N. Putilin, M. Marezio, S. Loureiro, J. J. Capponi, J. L. Tholence, A. Santoro, *Physica C* **1993**, *217*, 265.
[17] J. B. Goodenough, J. M. Longo, *Magnetic and Other Properties of Oxides and Related Compounds, Landolt-Börnstein, New Series, Group III, Vol. 4* (Eds.: K. H. Hellwege, O. Madelung), Springer, Berlin, **1970**.
[18] R. M. Kusters, D. A. Singleton, D. A. Keen, R. McGreevy, W. Hayes, *Physica B* **1989**, *155*, 362.
[19] R. von Helmolt, J. Wocker, B. Holzapfel, M. Schultz, K. Samwer, *Phys. Rev. Lett.* **1993**, *71*, 2231.
[20] K. Chahara, T. Ohno, M. Kasai, Y. Kozono, *Appl. Phys. Lett.* **1993**, *63*, 1990.
[21] H. L. Ju, C. Kwon, R. L. Greene, T. Venkatesan, *Appl. Phys. Lett.* **1994**, *65*, 2108.
[22] Y. Tokura, A. Urishibara, Y. Moritomo, T. Arima, A. Asamitsu, G. Kido, N. Furukawa, *J. Phys. Soc. Jpn.* **1994**, *63*, 3931.
[23] M. McCormack, S. Jin, T. H. Tiefel, R. M. Fleming, J. M. Phillips, *Appl. Phys. Lett.* **1994**, *64*, 3045.
[24] C. Zener, *Phys. Rev.* **1951**, *82*, 403.
[25] P. G. De Gennes, *Phys. Rev.* **1959**, *118*, 141.
[26] A. Maignan, C. Simon, V. Caignaert, B. Raveau, *Solid State Commun.* **1995**, *96*, 623; B. Raveau, A. Maignan, V. Caignaert, *J. Solid State Chem.* **1995**, *117*, 424.
[27] V. Caignaert, E. Suart, A. Maignan, C. Simon, B. Raveau, *C. R. Acad. Sci. Ser. IIa* **1995**, *321*, 515.
[28] Y. Tokura, *Colossal Magnetoresistive Oxides*, Gordon and Breach, New York, **1999**.
[29] *Colossal Magnetoresistance, Charge Ordering and Related Properties of Manganese Oxides* (Eds.: C. N. R. Rao, B. Raveau), World Scientific, Singapore, **1998**.
[30] Y. Tomioka, A. Asamitsu, Y. Moritomo, H. Kuwahara, Y. Tokura, *Phys. Rev. Lett.* **1995**, *74*, 5108.
[31] Y. Tomioka, A. Asamitsu, Y. Moritomo, Y. Tokura, *J. Phys. Soc. Jpn.* **1995**, *64*, 3626.
[32] Z. Jirák, S. Krupicka, V. Nekvasil, E. Pollert, G. Villeneuve, F. Zounova, *J. Magn. Magn. Mater.* **1980**, *15*, 519; Z. Jirák, S. Krupicka, V. Nekvasil, E. Pollert, G. Villeneuve, F. Zounova, *J. Magn. Magn. Mater.* **1985**, *53*, 153; E. Pollert, S. Krupicka, E. Kuzmicova, *J. Phys. Chem. Solids* **1982**, *43*, 1137.
[33] L. M. Rodriguez-Martinez, J. P. Attfield, *Phys. Rev. B* **1996**, *54*, R15622.
[34] B. Raveau, A. Maignan, C. Martin, *J. Solid State Chem.* **1997**, *130*, 162.
[35] B. Raveau, M. Hervieu, A. Maignan, C. Martin, *J. Mater. Chem.* **2001**, *11*, 29.
[36] C. Martin, A. Maignan, M. Hervieu, C. Autret, B. Raveau, D. Khomskii, *Phys. Rev. B* **2001**, *63*, 174402.

[37] P. V. Vanitha, A. Rulraj, A. R. Raju, C. N. R. Rao, *C. R. Acad. Sci.* **1999**, *2*, 595.
[38] V. Hardy, S. Hébert, A. Maignan, C. Martin, M. Hervieu, B. Raveau, *J. Magn. Magn. Mater.* **2003**, *264*, 183; A. Maignan, V. Hardy, C. Martin, S. Hébert, B. Raveau, *J. Appl. Phys.* **2003**, *93*, 7361.
[39] B. Raveau, D. Zhu, A. Maignan, M. Hervieu, C. Martin, V. Hardy, S. Hébert, *J. Phys. Condens. Matter* **2003**, *15*, 7055.
[40] B. Raveau, Md. Motin Seikh, *Cobalt Oxides. From Crystal Chemistry to Physics*, Wiley-VCH, Weinheim, **2012**.
[41] C. Martin, A. Maignan, D. Pelloquin, N. Nguyen, B. Raveau, *Appl. Phys. Lett.* **1997**, *71*, 1421; L. Barbey, N. Nguyen, V. Caignaert, F. Studer, B. Raveau, *J. Solid State Chem.* **1994**, *112*, 148.
[42] I. Terasaki, Y. Sasago, K. Ichinokura, *Phys. Rev. B* **1997**, R 12685.
[43] C. Fouassier, G. Metejka, J. M. Reau, P. Hagenmuller, *J. Solid State Chem.* **1973**, *6*, 532.
[44] P. Boullay, B. Domengès, M. Hervieu, D. Groult, B. Raveau, *Chem. Mater.* **1996**, *8*, 1482; P. Boullay, B. Domengès, M. Hervieu, D. Groult, B. Raveau, *Chem. Mater.* **1998**, *10*, 92; H. Leligny, D. Grebille, O. Perez, A. C. Masset, M. Hervieu, C. Michel, B. Raveau, *C. R. Acad. Sci. Ser. II Chim.* **1999**, *2*, 409; M. Hervieu, P. Boullay, C. Michel, A. Maignan, B. Raveau, *J. Solid State Chem.* **1999**, *142*, 305; H. Leligny, D. Grebille, O. Pérez, A. C. Masset, M. Hervieu, B. Raveau, *Acta Crystallogr. Sect. B* **2000**, *56*, 173; A. C. Masset, C. Michel, A. Maignan, M. Hervieu, O. Toulemonde, F. Studer, B. Raveau, *Phys. Rev. B* **2000**, *62*, 166.
[45] V. Caignaert, V. Pralong, V. Hardy, C. Ritter, B. Raveau, *Phys. Rev. B* **2010**, *81*, 094417; K. Singh, V. Caignaert, L. Chapon, V. Pralong, B. Raveau, A. Maignan, *Phys. Rev. B* **2012**, *86*, 024410.

